Influence of isotopic substitution on the anharmonicity of the interlayer shear mode of h-BN

Ramon Cuscó, James H. Edgar, Song Liu, Guillaume Cassabois, Bernard Gil, and Luis Artús

Influence of isotopic substitution on the anharmonicity of the interlayer shear mode of *h*-BN

Ramon Cuscó

Institut Jaume Almera (ICTJA-CSIC), Consejo Superior de Investigaciones Científicas,

Lluís Solé i Sabarís s.n., 08028 Barcelona, Spain

James H. Edgar and Song Liu

Department of Chemical Engineering,

Kansas State University, Manhattan, Kansas 66506, USA

Guillaume Cassabois

Laboratoire Charles Coulomb (L2C), UMR 5221

CNRS-Université de Montpellier, F-34095, Montpellier,France

Bernard Gil

Laboratoire Charles Coulomb (L2C), UMR 5221 CNRS-Université

de Montpellier, F-34095, Montpellier,France and

Ioffe Institute St. Petersburg, Polytekhnicheskaya 26, St. Petersburg, 194021, Russia.

Luis Artús

Institut Jaume Almera (ICTJA-CSIC), Consejo Superior de Investigaciones Científicas,

Lluís Solé i Sabarís s.n., 08028 Barcelona, Spain

Abstract

We present a detailed analysis of the temperature dependence of the interlayer shear mode that reveals a variation of the 4-phonon scattering coupling with isotopic mass. Phonon anharmonic decay and isotopic disorder effects are very weak for the low-energy interlayer shear mode, and the overall temperature dependence is mainly governed by the thermal lattice expansion. This allows us to observe systematic differences in the temperature dependence of the low energy mode with the isotopic mass that are related to the 4-phonon scattering contribution in quartic anharmonicity. The change in the quartic anharmonicity coefficient between the isotopically pure samples is larger than it would be purely expected from the mass variation.

I. INTRODUCTION

Hexagonal boron nitride (h-BN) is a layered crystal that is currently attracting a great deal of interest both from fundamental and applied points of view. Because of its unique properties, which combine high thermal conductivity with electrical insulating character in a lamellar structure similar to graphene, h-BN has acquired a prominent role as a dielectric in field-effect transistors based on stacked ultrathin layered materials held together by van der Waals forces.[1] h-BN was originally proposed as a promising candidate for ultraviolet laser applications following the demonstration of intense room-temperature lasing at 215 nm that was attributed to exciton emission.[2] Later studies have revealed however that h-BN is actually an indirect band gap semiconductor with conduction and valence extrema located at the M and K points, respectively.[3] Thus, phonons play a key role in determining the optical emission of h-BN, and, indeed, its emission spectra shows a rich fine structure of phonon assisted emission replicas.[3–5] In particular, phonon-assisted replicas involving up to six overtones of the interlayer shear mode (E_{2g}^{low}) have been reported in the emission spectra of h-BN at low temperature.[5]

Recently, isotopically purified h-BN has received much attention for its applications in high efficiency solid-state neutron detectors[6] and ultra-low loss phonon-polariton devices.[7,8] From a more fundamental standpoint, isotopical tuning of the van der Waals interaction and of the electron distribution between adjacent layers was demonstrated in isotopically purified h-BN,[9] opening prospects for future research on isotope engineered layered compounds. A good knowledge of the isotope and temperature dependence of the E_{2g}^{low} mode of h-BN, which is specific to the layered structure of this lamellar compound, is essential to advance our understanding of the subtle isotopic effects on van der Waals interactions. Very few studies of the temperature dependence of this mode exist in the literature. The temperature dependence of Raman spectra has provided a wealth of information about phonon decay channels and lifetimes in semiconductors of high current interest like InN.[10] In a previous work, we performed a temperature dependent anharmonicity analysis in natural composition h-BN and concluded that the anharmonic interactions of the E_{2g}^{low} mode are very small, the thermal downshift of this interlayer shear mode being primarily due to the lattice expansion along the c axis.[11] The temperature dependence of the E_{2g}^{low} mode has been used to monitor laser heating in Raman experiments on few-layer h-BN samples.[12]

Phonon studies on isotopic dependence are even more scarce. In a recent publication,[13]

2

we analyzed the isotopic effects on the phonon anharmonic decay of the high-energy Raman-active mode of h-BN. Changes in the main decay pathways were established as a result of the sizable isotopic shift of the upper optical phonon branches.[13] Since the isotopic shifts are very small for the low lying branches, such dramatic effects are not expected in the low-energy Raman active mode. Nevertheless, the interlayer shear mode is particularly sensitive to the van der Waals forces and may be influenced by subtle isotopic effects.[9]

The predominant role of the 4-phonon scattering mechanism of quartic anharmonicity in layered compounds has been well established for the high-frequency mode both in graphite[14,15] and h-BN.[13] However, since phonon anharmonic decay and isotopic disorder have also a significant influence on the high-frequency mode, it is difficult to single out the effects of isotopic substitution on this anharmonic mechanism from the analysis of the experimental temperature dependence data. In contrast, both the phonon anharmonic decay and isotopic disorder effects are negligibly small for the E_{2g}^{low} mode, which makes it possible to directly relate the variations in the temperature dependence of the E_{2g}^{low} frequency with the isotopic mass to variations in the 4-phonon scattering contribution.

Here we present a detailed investigation of the isotopic effects on the temperature dependence of the E_{2g}^{low} mode in isotopically pure h-BN by means of high-resolution Raman scattering. The separate contributions of the lattice thermal expansion and phonon anharmonicity are evaluated with the aid of first principle calculations, giving insight into the relative importance of these effects and of the influence of isotopic substitution.

II. EXPERIMENT

The isotopically enriched hexagonal boron nitride crystals were grown from high-purity elemental ^{10}B (99.2 at%) or ^{11}B (99.4 at%) powder by using metal flux method. A Ni-Cr-B powder mixture at respective 48, 48, 4 wt% was loaded into an alumina crucible and placed in a single zone furnace. The furnace was evacuated and then filled with N_2 and forming gas (5% hydrogen in balance argon) to a constant pressure of 850 Torr. During the reaction process, the N_2 and forming gases continuously flowed through the system with rates of 125 sccm and 25 sccm, respectively. All the nitrogen in the h-BN crystal originated from the flowing N_2 gas. The forming gas was used to minimize oxygen and carbon impurities in the h-BN crystal. After a dwell time of 24 hours at 1550 °C, the h-BN crystals were precipitated on the metal surface by cooling

at a rate of 1 °C/h to 1500°C, and then the system was quickly quenched to room temperature. Natural isotopic composition (20% ^{10}B and 80% ^{11}B) h-BN crystals were prepared by using a 50 wt% Ni and 50 wt% Cr mixure loaded into a hot-pressed boron nitride ceramic boat which served as soured material. The growth procedure was the same as described above.

Measurements from RT down to 80 K were carried out in a TBT-Air Liquide liquid nitrogen (LN$_2$) cryostat equipped with a platinum resistance sensor and a temperature controller. For the high temperature measurements, a Linkam THMS600 heating stage was employed. Great attention was given to achieving good thermal contact and accurate temperature readings from a thermocouple close to the sample location (for details on sample mounting, see Ref. 11). The Raman scattering measurements were carried out in backscattering configuration from the c face using the 632.82-nm line of a He-Ne laser. The scattered light was analyzed using a Jobin-Yvon T64000 triple spectrometer equipped with a LN$_2$-cooled charge-coupled device (CCD) detector. The Raman spectra were recorded using the subtractive configuration of the spectrometer with 60-μm slits, which corresponds to a spectral bandwidth of $\sim$ 1 cm^{-1}. To improve the peak definition, the Raman spectra of the extremely narrow E_{2g}^{low} mode were tightly sampled by merging up to seven different spectra taken at slightly different grating positions. For an accurate determination of the Raman frequency, the spectra were calibrated against the 638.299 nm emission line of a Ne lamp. The laser power on the sample was kept very low to avoid heating effects.

First-principle phonon calculations were performed in the framework of density functional perturbation theory in the local density approximation as implemented in the ABINIT package.[16] Calculation details and the underlying theory used to evaluate the thermal expansion, anharmonicity, and isotopic disorder effects are given in Ref. 13.

III. RESULTS AND DISCUSSION

Figure 1 (a) shows representative Raman spectra of the E_{2g}^{low} mode for ^{10}BN,^{11}BN, and natural isotopical composition samples recorded at 80 and 300 K. The circles correspond to experimental points whereas the solid lines are Gaussian line shape fits. The latter display a linewidth equal to the spectrometer bandwidth as determined from a measurement of the 638.3-nm Ne line. This indicates that the linewidth Γ of the E_{2g}^{low} mode is significantly lower than the spectrometer bandwidth. Only a slight linewidth increase $\Delta\Gamma \sim 0.1$ cm^{-1} is observed at room tem-
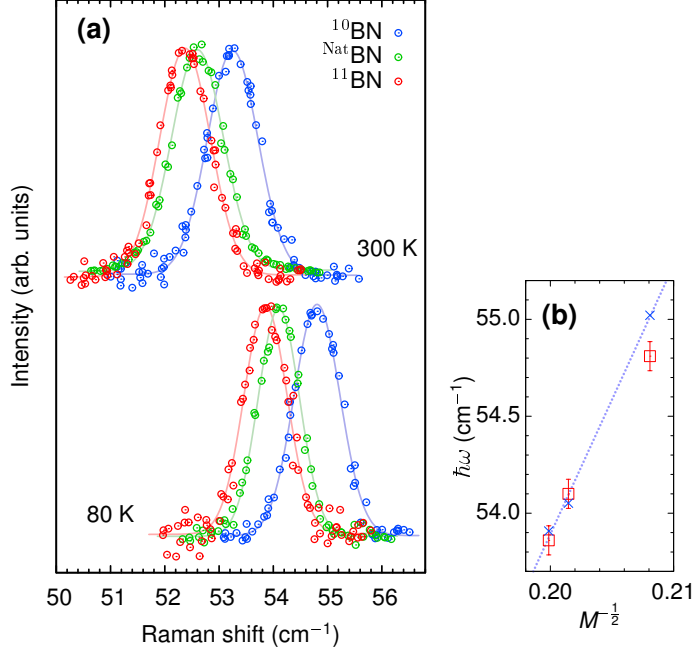
FIG. 1. (a) High-resolution Raman spectra of the E_{2g}^{low} mode for isotopically pure and natural composition h-BN samples at 80 and 300 K. Circles are experimental data points merged from separate spectra recorded with a slight shift in the grating position. Solid lines are Gaussian line-shape fits to the experimental points. (b) Frequency of the E_{2g}^{low} interlayer shear mode at 80 K vs. the square root of the formula-unit mass (squares). The crosses are the corrected values derived from DFT calculations and the dotted line indicates the expected linear scaling of the shear mode with the inverse square root of the mass.

perature, consistent with previously reported results on natural compositon h-BN.[11]

The isotopic-disorder induced broadening is proportional to the square of the phonon frequency and to the phonon density of states.[13,17] As a consequence, the effects of isotopic broadening, which are on the order of 2 cm^{-1} for the high-energy E_{2g}^{high} mode,[13] are completely negligible in the case of the E_{2g}^{low} mode, as it has an energy about 30 times smaller and a very low phonon density of states. This is expected since the E_{2g}^{low} shear mode involves the rigid gliding motion of adjacent hexagonal layers which can be considered as homogeneous planes with an average isotopic mass. Indeed, no linewidth variation can be observed in Fig. 1 (a) between the natural composition sample and the isotopically pure samples.

The shear mode frequency increases by ∼ 1 cm^{-1} from ^{11}BN to ^{10}BN. Because of the rigid gliding motion of the layers, the E_{2g}^{low} mode frequency is expected to scale as the inverse square

root of the formula-unit mass. In Fig. 1 (b) we plot the E_{2g}^{low} frequencies at 80 K and the calculated DFT values, vertically shifted to match the experimental results, vs. the inverse square root of the formula-unit mass. While the calculated points (blue crosses) and the frequencies measured on the ^{11}BN and natural composition samples follow the linear scaling with $M^{-\frac{1}{2}}$, the E_{2g}^{low} frequency measured on the ^{10}BN sample lies below the expected value. The experimental measurements reveal an apparent softening of the E_{2g}^{low} mode in ^{10}BN that could be related to a more diffuse electron distribution between adjacent layers previously reported in isotopically pure ^{10}BN samples.[9]

Anharmonic interactions of the E_{2g}^{low} mode were determined to be very weak in natural composition h-BN on account of the lack of available decay channels for such a low energy mode.[11] Taking into account that isotopic substitution does not affect significantly the lower energy phonon branches,[13] the same situation should hold in isotopically pure samples. This is consistent with the linewidth of the Raman peaks shown in Fig. 1 (a), where the FWHM increase between 80 K and room temperature (~ 0.1 cm^{-1}) lies within experimental error. Then, the substantial downshift of the E_{2g}^{low} mode with increasing temperature that is observed in Fig. 1 (a) must be due to the thermal expansion of the interlayer distance. Thermal expansion coefficients can be calculated in the quasi-harmonic approximation by considering a temperature-dependent contribution to the free energy due to phonons. A derivation of the thermal expansion coefficients for an anisotropic crystal is given in Ref. 13.

They can be expressed as

$$\alpha_a = \frac{k_B}{V_0} \sum_{\mathbf{q},j} \left(\frac{\hbar \omega_{\mathbf{q},j}}{2 k_B T} \right)^2 \text{csch}^2 \left(\frac{\hbar \omega_{\mathbf{q},j}}{2 k_B T} \right) [(S_{11} + S_{12}) \gamma_a(\mathbf{q}, j) + S_{13} \gamma_c(\mathbf{q}, j)] \tag{1}$$

$$\alpha_c = \frac{k_B}{V_0} \sum_{\mathbf{q},j} \left(\frac{\hbar \omega_{\mathbf{q},j}}{2 k_B T} \right)^2 \text{csch}^2 \left(\frac{\hbar \omega_{\mathbf{q},j}}{2 k_B T} \right) (2 S_{31} \gamma_a(\mathbf{q}, j) + S_{33} \gamma_c(\mathbf{q}, j)), \tag{2}$$

where S_{ij} are the elastic compliance tensor elements, γ_a and γ_c are, respectively, the *in-plane* and *out-of-plane* Grüneisen parameters, and the heat capacity $c_v(\omega_{\mathbf{q},j})$ is given by

$$c_v(\omega_{\mathbf{q},j}) = \left(\frac{\hbar \omega_{\mathbf{q},j}}{2 k_B T} \right)^2 \text{csch}^2 \left(\frac{\hbar \omega_{\mathbf{q},j}}{2 k_B T} \right). \tag{3}$$

Here, k_B is the Boltzmann constant and $\hbar$ is Planck's constant. Eqs. (1) and (2) describe accurately the temperature dependence of the lattice parameters a and c measured by x-ray diffraction.[18] However, since the temperature-independent zero-point and structural contributions were ignored, this approach does not give information about the volume dependence
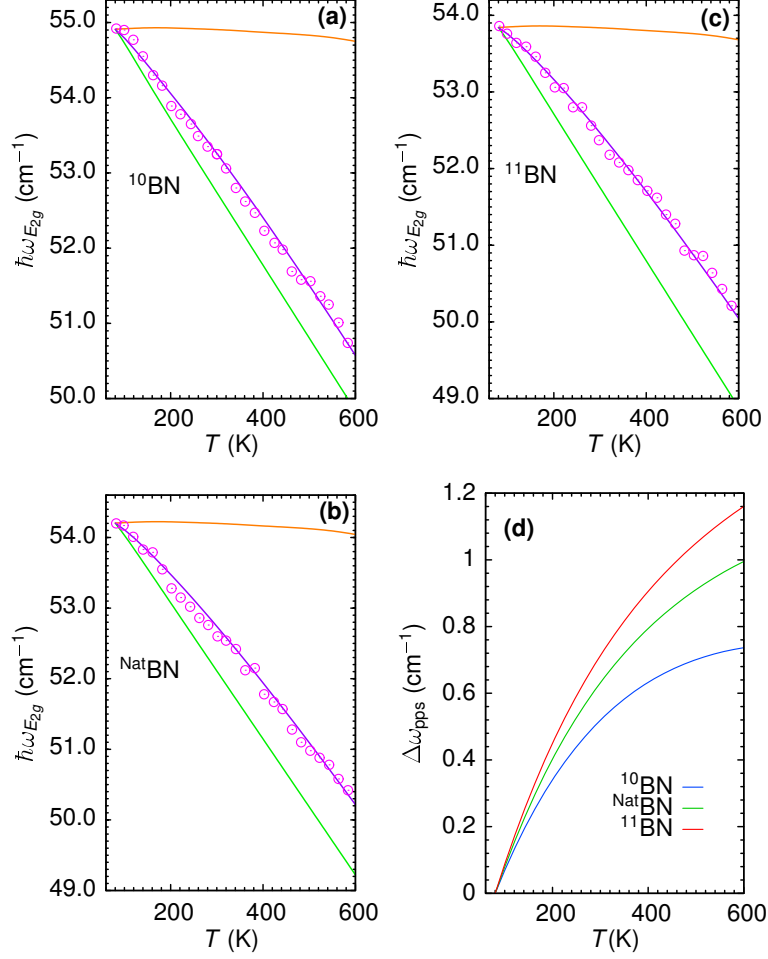
FIG. 2. (a) to (c) Temperature dependence of the E_{2g}^{low} frequency (circles) for ^{10}BN, $^{\text{Nat}}$BN, and ^{11}BN samples. The green line is the thermal expansion contribution calculated in the quasi-harmonic approximation. The orange line depicts the small anharmonic decay contribution, whereas the violet line was fitted to the data by considering all the above contributions plus a quartic phonon-phonon scattering term (see text). (d) Frequency shift due to phonon-phonon scattering for the three crystals with different isotopic compositions.

on the isotopic mass. Given that the ABINIT code used here determines the equilibrium lattice constant in the harmonic approximation, it yields the same lattice constant irrespective of the isotopic mass. Calculations performed on isotropic cubic semiconductors suggest that the lattice constant variations with isotopic mass are small.[19] Therefore, we will neglect this effect and attempt to model only temperature variations of the E_{2g}^{low} frequency relative to the values at 80 K originating in anharmonic interactions.

The temperature dependence of the E_{2g}^{low} mode in the 80–600 K range is plotted in Fig. 2 for

the three different isotopic samples studied. The small anharmonic decay shift is not expected to depend significantly on isotopic mass and it is evaluated in all cases from the effective anharmonic potential $|V_3^-|^2 = 5.4$ cm^{-2} determined for ^{Nat}BN in Ref. 11, which corresponds to an upconversion difference channel $E_{2g}^{low}(\Gamma) \rightarrow A_{2u}(M) - TA(M)$. The resulting anharmonic decay shift is displayed in Figs. 2 (a) to (c) as an orange line and is virtually null. The thermal expansion contribution to the E_{2g}^{low} frequency is depicted in Figs. 2 (a) to (c) by a green line. This is obtained from DFT calculations of the phonon frequency that take into account the temperature variation of the lattice constants determined by integration of Eqs. (1) and (2). Note that the calculated frequencies have been corrected to match the experimental point at 80 K. While the magnitude of the thermal expansion contribution may explain the observed E_{2g}^{low} frequency downshift with temperature, the latter is consistently lower than expected in all three isotopical samples, the deviation being highest for the ^{11}BN sample and smallest for the ^{10}BN sample [see Figs. 2 (a) to (c)].

These discrepancies can be resolved if the quartic anharmonic correction due to 4-phonon scattering is taken into account. We showed that the anharmonic coupling to the low-lying modes through 4-phonon scattering plays a prominent role in layered compounds like h-BN, where the temperature dependence of the high-energy E_{2g} mode is mainly governed by this mechanism.[11] The 4-phonon scattering contribution to the frequency shift can be approximated by[11]

$$\Delta_i^{4ps} \approx \frac{1}{2\hbar} \sum_j \int_{\omega_j}^{\omega_{j+1}} d\omega \frac{\partial^4 E}{\partial u_i^2 \partial u_j^2} [2n(\omega) + 1] \rho(\omega), \tag{4}$$

where the sum runs over all phonon branches, E is the interatomic potential energy, and u_j are adimensional phonon displacements. The coupling potentials $V^{4ps} = \partial^4 E/\partial u_i^2 \partial u_j^2$ are assumed to be dispersionless and are evaluated at zone-center from *ab-initio* calculations. In layered compounds, it is the coupling to the lowest-lying branches –which have higher occupation factors– what primarily determines the frequency correction. In the case of the high-energy E_{2g} mode, the 4-phonon scattering coupling potential to the lowest-lying E_{2g}^{low} mode is negative, whereas the coupling is positive but very small for the B_{1g}^{low} mode,[11] giving a large negative correction. In contrast, the coupling coefficient of the E_{2g} shear mode to itself is large and positive, whereas coupling coefficients to all other higher energy modes are negative. This results in partial cancellation of the 4-phonon scattering effects, with a net correction that is much smaller than in the case of the high-energy E_{2g} mode and positive.

8

To model these compensating effects, we consider a piecewise average effective anharmonic potential defined as

$$\tilde{V}^{4\mathrm{ps}}(\omega) = \begin{cases} \tilde{V}_+^{4\mathrm{ps}} & \omega \le \omega_c \\ \tilde{V}_-^{4\mathrm{ps}} & \omega > \omega_c, \end{cases}$$

where the crossover frequency ω_c is chosen at the midpoint between the two lowest zone-center modes (see Refs. 11 and 13), and we fit the experimental data including the additional 4-phonon scattering shift

$$\Delta_{T_0}^{4\mathrm{ps}}(T) = \int_0^\infty d\omega \, \tilde{V}^{4\mathrm{ps}}(\omega)[n(\omega, T) - n(\omega, T_0)]\rho(\omega). \tag{5}$$

Here $n(\omega, T)$ is the Bose-Einstein factor, $\rho(\omega)$ is the phonon density of states, and the shift $\Delta_{T_0}^{4\mathrm{ps}}(T)$ is evaluated relative to the 4-phonon scattering correction at temperature $T_0 = 80$ K. As can be seen in Figs. 2 (a)–(c), the ^{10}BN, $^{\mathrm{Nat}}$BN, and ^{11}BN data are nicely fitted using the potentials $\tilde{V}_+^{4\mathrm{ps}} = 3.2, 3.4, 3.7$ cm^{-1} and $\tilde{V}_-^{4\mathrm{ps}} = -0.38 - 0.38, -0.40$ cm^{-1}, respectively. These results indicate that the anharmonic 4-phonon scattering interaction is strongest with the low energy acoustic phonon branches. This difference in anharmonic coupling is plausible given the quasi-acoustic nature of the interlayer shear mode. In fact, the E_{2g}^{low} mode can be viewed as a zone folding of the *in-plane* acoustic branches along the Γ-A direction resulting from the alternate layout of B and N atoms along the c direction.

As the effect of the isotopic mass on the temperature dependence of the lattice parameters has been included in the evaluation of the thermal expansion shifts shown as green lines in Fig. 2 (a) to (c), and the anharmonic decay and isotopic disorder contributions are negligible, the difference between the experimental points and the thermal expansion shift that can be seen in Fig. 2 must arise from the 4-phonon scattering in quartic anharmonicity. In Fig. 2 (d) we plot the separate contribution of the 4-phonon scattering to the shear-mode frequency shift. A small positive shift is found for all samples, which tends to saturate at high temperatures as the phonon occupation in higher energy phonon branches increases and compensates the anharmonic interaction with the lower energy acoustic branches. Interestingly, the magnitude of the 4-phonon correction gradually increases with the boron isotopic mass, indicating an enhancement of the 4-phonon scattering mechanism by isotopic substitution.

A purely dynamical increase of the quartic anharmonicity coefficients $V^{4\mathrm{ps}} = \partial^4 E / \partial u_i^2 \partial u_j^2$ in the crystals with the heavier boron isotope arises from the dependence on the inverse square

9

root of the phonon frequencies of the derivatives with respect to the adimensional phonon displacements.[20] An estimate of the magnitude of this effect can be obtained by considering the relation between the $V^{4\text{ps}}$ coefficients and the Fourier components of the interatomic potential introduced by Born and Huang[21], which is given by[22]

$$V^{4\text{ps}} \equiv V^4(\boldsymbol{q}j; -\boldsymbol{q}j; \boldsymbol{q}_1 j_1; -\boldsymbol{q}_1 j_1) = \frac{\Phi(\boldsymbol{q}j; -\boldsymbol{q}j; \boldsymbol{q}_1 j_1; -\boldsymbol{q}_1 j_1)}{\omega(\boldsymbol{q}, j)\omega(\boldsymbol{q}_1, j_1)}. \tag{6}$$

Taking into account that the 4-phonon scattering mechanism is dominated by the lowest frequency phonons, an estimation of the effect of the isotopic shift on the $V^{4\text{ps}}$ coefficients can be obtained from Eq. (6) by assuming $\omega(\boldsymbol{q}, j) \approx \omega(\boldsymbol{q}_1, j_1) \approx \omega_{E_{2g}^{\text{low}}}$. Then, the expected increase of the anharmonic coefficient due to the mass effect on the phonon frequencies between the boron-10 and boron-11 isotopically pure crystals can be estimated by

$$\Delta_M V_+^{4\text{ps}} \approx \left[\left(\frac{\omega_{E_{2g}^{\text{low}}}^{^{10}\text{BN}}}{\omega_{E_{2g}^{\text{low}}}^{^{11}\text{BN}}} \right)^2 - 1 \right] V_+^{4\text{ps}}(^{10}\text{BN}). \tag{7}$$

At 80 K, the shear mode frequency $\omega_{E_{2g}^{\text{low}}}$ is measured at 54.81 and 53.86 cm^{-1} for ^{10}BN and ^{11}BN, respectively. Then, Eq. (7) yields $\Delta_M V_+^{4\text{ps}} \sim 0.1$ cm^{-1}, which is only $\sim 20\%$ of the increase of the effective 4-phonon potentials derived from the analysis of the Raman data (0.5 cm^{-1}). This suggests that isotopic substitution has an influence on the anharmonic interactions of the shear mode, consistent with previous reports of a modified interlayer electronic distribution in isotopically purified ^{10}BN.[9]

A full theoretical treatment of isotopic effects on the non-local interlayer interactions and their impact on the shear mode frequency would be required to ascertain the origin of the observed behavior. Such a treatment is beyond the scope of the present work. Nevertheless, the systematic variation of the temperature dependence of the shear mode frequency reported here clearly suggests that dynamical phonon properties can be altered by isotopic substitution.

IV. CONCLUSIONS

Detailed temperature-dependent, high-resolution Raman scattering measurements of the interlayer shear mode on isotopically pure h-BN crystals and *ab-initio* calculations have revealed subtle changes in the phonon dynamics, namely in the anharmonic mechanisms that determine the temperature dependence of phonons in layered crystals. This is the first demonstration that isotope engineering can modulate phonon features beyond the trivial change of

frequency. The negligible effects of phonon anharmonic decay and isotopic disorder on the low-frequency shear mode single out the 4-phonon scattering mechanism in quartic anharmonicity as the source of anharmonic correction to the temperature dependence of the shear mode. The analysis of the Raman measurements suggests an increasing contribution of the 4-phonon scattering with isotopic mass. Similar effects should be expected in other lamellar compounds featuring low-energy interlayer shear modes. The mass variation between the isotopically pure h-BN samples cannot account on its own for the observed increase of the quartic anharmonicity coefficients, which suggests that other mechanisms affecting anharmonic interactions in isotopically substituted samples should be contemplated. Our experimental results highlight temperature dependent Raman measurements as a powerful probe of anharmonic interactions and may stimulate further theoretical studies of anharmonic phonon interactions in layered compounds.

[1] C. R. Dean, A. F. Young, I. Meric, C. Lee, L. Wang, S. Sorgenfrei, K. Watanabe, T. Taniguchi, P. Kim, K. L. Shepard, et al., Nat. Nanotechnol. **5**, 722 (2010).

[2] K. Watanabe, T. Taniguchi, and H. Kanda, Nat. Mater. **3**, 404 (2004).

[3] G. Cassabois, P. Valvin, and B. Gil, Nat. Photonics **10**, 262 (2016).

[4] G. Cassabois, P. Valvin, and B. Gil, Phys. Rev. B **93**, 035207 (2016).

[5] T. Q. P. Vuong, G. Cassabois, P. Valvin, V. Jacques, R. Cuscó, L. Artús, and B. Gil, Phys. Rev. B **95**, 045207 (2017).

[6] A. Maity, T. C. Doan, J. Li, J. Y. Lin, and H. X. Jiang, Appl. Phys. Lett. **109**, 072101 (2016).

[7] T. Low, A. Chaves, J. D. Caldwell, A. Kumar, N. X. Fang, P. Avouris, T. F. Heinz, F. Guinea, L. Martin-Moreno, and F. Koppens, Nat. Mater. **16**, 182 (2016).

[8] A. J. Giles, S. Dai, I. Vurgaftman, T. Hoffman, S. Liu, L. Lindsay, C. T. Ellis, N. Assefa, I. Chatzakis, T. L. Reinecke, et al., Nature Mater. **17**, 134 (2018).

[9] T. Q. P. Vuong, S. Liu, A. van de Lee, R. Cuscó, L. Artús, T. Michel, P. Valvin, J. H. Edgar, G. Cassabois, and B. Gil, Nat. Mater. **17**, 152 (2018).

[10] N. Domènech-Amador, R. Cuscó, L. Artús, T. Yamaguchi, and Y. Nanishi, Phys. Rev. B **83**, 245203 (2011).

[11] R. Cuscó, B. Gil, G. Cassabois, and L. Artús, Phys Rev B **94**, 155435 (2016).

[12] I. Stenger, L. Schué, M. Boukhicha, B. Berini, B. Plaçais, A. Loiseau, and J. Barjon, 2D Mater. **4**, 031003 (2017).

[13] R. Cuscó, L. Artús, J. E. Edgar, S. Liu, G. Cassabois, and B. Gil, Phys. Rev. B **97**, 155435 (2018).

[14] N. Bonini, M. Lazzeri, N. Marzari, and F. Mauri, Phys. Rev. Lett. **99**, 176802 (2007).

[15] P. Giura, N. Bonini, G. Creff, J. B. Brubach, P. Roy, and M. Lazzeri, Phys. Rev. B **86**, 121404(R) (2012).

[16] ABINIT is a common project of the Université Catholique de Louvain, Corning Incorporated, and other contributors (http://www.abinit.org). X. Gonze, J.-M. Beuken, R. Caracas, F. Detraux, M. Fuchs, G.-M. Rignanese, L. Sindic, M. Verstraete, G. Zerah, F. Jollet, et al., Comput. Mater. Sci. **25**, 478 (2002).

[17] S. Tamura, Phys. Rev. B **30**, 849 (1984).

[18] W. Paszkowicz, J. Pelka, M. Knapp, T. Szyszko, and S. Podsiadlo, Appl. Phys. A **75**, 431 (2002).

[19] A. Debernardi and M. Cardona, Phys. Rev. B **54**, 11305 (1996).

[20] L. Paulatto, F. Mauri, and M. Lazzeri, Phys. Rev. B **87** (2013).

[21] M. Born and K. Huang, *Dynamical Theory of Crystal Lattices* (Oxford: Clarendon Press, 1954).

[22] A. A. Maradudin and A. E. Fein, Phys. Rev. **128**, 2589 (1962).